

## 2. Amplification of climate change in mountains

E. Palazzi<sup>1</sup>

<sup>1</sup>*CNR-ISAC, National Research Council of Italy, Institute of Atmospheric Sciences and Climate, Torino, Italy*

### 2.1 Elevation-dependent warming (EDW)

The average global temperature on Earth has increased of about 1°C since 1880, the time around which the measuring stations started to sufficiently cover enough of the planet to have reliable and homogeneous temperature records. The global temperature mainly depends on the balance between the energy that the planet receives from the Sun and the energy it radiates back to space. The latter is significantly affected by the chemical composition of the atmosphere, particularly by the amount of greenhouse gases such as water vapor, carbon dioxide, methane, nitrous oxide and others which are able to absorb and re-emit part of the terrestrial radiation. The naturally occurring concentrations of greenhouse gases, resulting from their exchange between the various components of the climate system and from their transformations through the biogeochemical cycles, give rise to the natural greenhouse effect, which has basically allowed the average surface temperature of the planet to reach values suitable for life.

Two-thirds of the warming occurred during the last ~150 years has occurred since 1975, at a rate of roughly 0.15-0.20°C per decade, in response to the likewise rapid increase of greenhouse gases. These are a product of human activities like burning of fossil fuels, vehicular traffic, industrial processes, as well as changes in land cover and land use, like deforestation or urbanization. The most important greenhouse gases whose concentration has increased in response to human activities are carbon dioxide, methane, and nitrous oxide. The increase of greenhouse gas concentrations in the atmosphere well above their natural levels has led to an amplification of the natural greenhouse effect. Water vapour, the most important natural greenhouse gas on Earth, is not directly emitted by human activities but its concentration nevertheless increases in a warmer world, which activates a powerful positive feedback enhancing the initial warming.

It is worth stressing that a one-degree temperature increase, averaged over the globe, is a significant amount for at least two reasons. One is that it takes a vast amount of additional heat stored in the different Earth system components to warm the oceans, the atmosphere, and the land by that much. The other is that such an averaged amount translates into a temperature increase which can differ a lot from region to region. Warming is not uniform across the globe indeed. An example is provided in Figure 1 showing the January 2018 temperature anomaly, calculated with respect to the 1951-1980 baseline climatology, from the NASA/GISS/GISTEMP data (Hansen et al., 2010). This dataset combines the data acquired by about 6,300 meteorological stations around the world, ship- and buoy-based instruments measuring sea surface temperature, and Antarctic research stations. Surface warming is generally greater over land than over the oceans because water absorbs and releases heat slowly (thermal inertia) and because the heat stored in oceans has to be distributed over a mass which is much greater for oceans than for the atmosphere. Moreover, some land areas have warmed more (and faster) than others or compared to the globally-averaged temperature increase. One generally refers to these areas as “hot-spot” or “sentinel” regions. Hot-spots, not only

because they undergo greater warming rates than the rest of the globe, but also because of the amplified impacts of such warming as well as for the importance which they cover in the global climate system. Sentinels, owing to their “ability” of showing early and in an amplified way what the effects of a temperature increase would be. These areas include the coldest regions of the World, like the Arctic (Serreze and Francis, 2006) and the high-altitude mountain regions (Pepin et al., 2015).

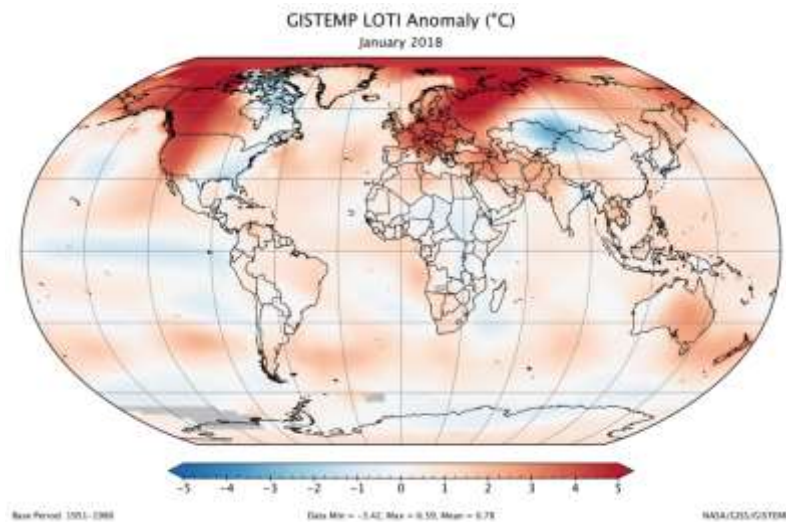


**Figure 1.** Global map of the January 2018 LOTI (land-ocean temperature index) anomaly relative to the 1951-1980 January climatology (NASA/GISS/GISTEMP data, [www.giss.nasa.gov](http://www.giss.nasa.gov)).

Amplified warming in the Arctic - broadly accepted to result from feedback loops such as the snow/ice-albedo feedback (Chapin et al., 2005) – has been referred to as “Arctic Amplification” (Serreze and Barry, 2011). High-altitude mountain regions resemble high latitudes in terms of climatic conditions - both are cold and dry environments - and the feedback loops which are at play, first of all, the ice/snow albedo feedback. On the other hand, the high elevation areas have overall more complex climate patterns than the Arctic, for a twofold reason. Because mountains host more heterogenous landscapes and are characterized by a variety of micro-climates (Barry, 2008) and because they are not limited to one geographical area like the Arctic, but they are sparse in all climatic zones of the world for the tropics to the temperate and polar areas.

Even ignoring external forcing factors impinging upon mountains such as land use/cover changes and climate and environmental changes, features like topography, slope, aspect and exposure alone would make the temperature and other meteo-climatic variables measured in mountain regions characterized by extreme local variability. All this makes it difficult to study climate processes in mountains overall, and to understand the mechanisms driving warming rates in high-altitude regions when trying to provide a picture able to describe all mountain regions of the World.

Notwithstanding these intrinsic difficulties and the many factors which concur in limiting our ability to determine the rate of warming in mountainous regions (see Sect. 2.2), the analysis of available observations, corroborated by climate model results, points toward an amplification of warming rates in mountain areas, similar to the Arctic Amplification, a phenomenon which has been referred to as “Elevation-Dependent Warming” (EDW). This means that high-mountain environments would

experience more rapid changes in temperature than their counterparts at lower elevations, or compared to globally-averaged temperature increase.

Elevation-dependent warming has important implications for the mass balance of the high-altitude cryosphere leading to consequences on the storage of water in its reservoirs and on future water availability. Amplified warming in mountains affect local ecosystems and biodiversity, as well as downstream societies.

In this chapter, we review the definition of EDW, its evidence in observations and in model simulations, along with the uncertainties which accompany EDW assessment. We also illustrate the mechanisms that have been proposed to account for this phenomenon in the different mountain regions of the World. We will discuss all this mostly using a global perspective, but we will provide also a special focus on the Alpine region, particularly exploiting the results of one study published under the umbrella of the NextData project, which compares the characteristics of EDW in the Greater Alpine Region (encompassing the Italian Alps) compared to other two mountain ranges of the Northern Hemisphere located in the same latitude band. The open issues, the strategy for future research on this topic, and link to existing relevant Initiative are also discussed at the end of the chapter.

## **2.2 Methodological approaches to the study of EDW**

The correct, literal acronym of EDW - elevation-dependent warming - would not imply that the rate of warming increases with elevation, but that it depends on elevation. The very important intrinsic requirement to deal with EDW would be that there is a statistically significant rate of warming (which implies having measurements for a sufficiently long time period, at least 20-30 years) and that this rate of warming is not constant with elevation.

In the majority of EDW studies, the warming rate is quantified using long surface (minimum and maximum) temperature time series and extracting the magnitude of the temporal trend. Sometimes, as an alternative to the calculation of the trend, the temperature change is considered, calculated as the difference between the average of temperature over 20-30 years at the end of the time period which is considered and the average of temperature over 20-30 years at the beginning of that period, provided that the temperature record is long enough.

The second step is to assess whether the calculated warming signal (either as trend or change) exhibits a dependence on elevation. As commonly done in the literature (e.g. Liu and Chen, 2000; Vuille et al., 2003; Pepin and Lundquist, 2008; Liu et al., 2009; Qin et al., 2009; Rangwala et al., 2010; Palazzi et al., 2017), this is done by calculating the slope obtained by linear regression of the temperature trends (or changes) against the elevation. The regression can be performed both at each grid point (for gridded observational datasets, reanalysis products and model data) or location (for station data) and using data averaged into elevational bands. The statistical significance of the linear slopes is then assessed, which can be done using different methods.

When the rate of the temperature trend/change is found to exhibit a statistically significant relationship with elevation, we can say we are in presence of EDW. This can be defined either for the whole globe or regionally or within a single mountain range. In principle, the slope does not have to be positive or negative (according to the literal definition of EDW), or necessarily linear

(which is not often the case, indeed), but it does have to be systematic. Despite these premises, it is worth stressing that, in the literature, EDW is more often associated with an increase of warming rates with elevation, i.e. the slope describing the relationship between warming rates and elevation is positive.

Some studies showed that the relationship may not be linear instead, but it can exhibit a different behavior if evaluated in different elevational bands within a given mountain range (e.g. Palazzi et al., 2017, 2019). It is also recommended to deal with EDW in the minimum and maximum temperature separately, since different mechanisms driving an amplification of warming rates can act differently during daytime and nighttime.

For clarity, Figure 2 illustrates through an example taken from the model study by Palazzi et al. (2017) the common procedure to assess EDW. That study uses an ensemble of the latest generation global climate models (GCMs) - the Climate Model Intercomparison Project Phase 5 (CMIP5) GCMs - to assess historical and future EDW in one region exhibiting the most outstanding evidence of EDW in observations, i.e. the Himalayas-Tibetan Plateau (e.g. Pepin et al., 2015 and references therein). Figure 2a shows the topographic map of the investigated area from a high-resolution digital elevation model while Figure 2b show how much smoother is the topography of the area seen by the ensemble mean of the employed GCMs. Figure 2c shows the change between the period 2071-2100 (end of the 21st century) and the period 1971-2000 (end of the 20th century) of the minimum temperature over the study area, while Figure 2d relates this change to surface elevation. This example refers to the winter period (December-January-February, DJF) and the future projections are evaluated under the highest emission scenario, RCP8.5 (Riahi et al., 2011), belonging to the generation of scenarios ([http://sedac.ipcc-data.org/ddc/ar5\\_scenario\\_process/RCPs.html](http://sedac.ipcc-data.org/ddc/ar5_scenario_process/RCPs.html)) used in the 2013 IPCC Assessment Report (AR5, IPCC, 2013). The slope of linear regression (in °C/km) is indicated in Figure 2d (both calculated over the entire range of elevations, in red, and from 500 m a.s.l. upwards, in blue). A star symbol in parentheses indicates the statistical significance of the elevational trend of the minimum temperature change (for details see Palazzi et al., 2017).

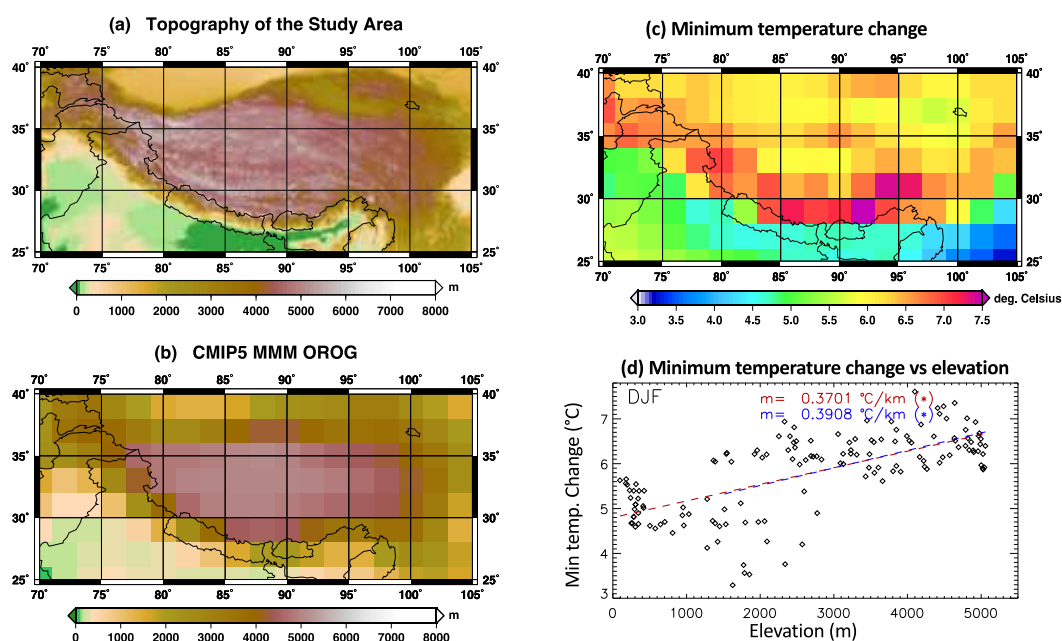


**Figure 2.** Example to illustrate a methodology to assess and quantify EDW (see text for details). Panels a, b and d are from Palazzi et al., (2017).

## **2.3 Evidence of EDW, with a focus on the Alpine region**

EDW has been studied using in-situ measurements, satellite and reanalysis data as well as model simulations. Each kind of data has advantages and limitations, which will be more deeply addressed in Sect. 2.4. Most studies conducted so far have been performed using in situ observations of minimum and maximum temperatures and climate model simulations, both regional and global models, especially when investigating and trying to disentangle the mechanisms driving EDW. Observational studies are in less agreement with each other than model simulations. A majority of studies based on observations, in fact, suggest that warming is more rapid at higher elevations but a number of them also show an opposite behaviour or no relationship or even a more complex situation with, e.g., no significant elevational gradient but highest warming rates at intermediate elevations (see Table 1 of Pepin et al., 2015 and references therein for details). Most models integrate trends over a long time period (typically up to the end of the 21st century) when EDW is expected to become more widespread than it has been so far. This makes their picture of historical and future EDW more coherent between the different studies employing model simulations than between observational studies. Sections 2.3.1 and 2.3.2 discuss the evidence of EDW in observations and in model simulations, as from the current literature.

### **2.3.1 Evidence of EDW in Observations**

We will discuss in detail in Sect. 2.4 what factors make it difficult to measure and document, using different kinds of observing systems, the rate and geographical pattern of warming in mountainous regions. Here we focus rather on the results of the main observational studies on EDW in the different high-elevation regions of the world, summarizing the literature as a whole and providing a focus on the Alpine Region.

One of the first studies on EDW at the global scale was performed by Diaz and Bradley (1997) who analysed the minimum and maximum temperature time series, from 1951 to 1989, at 126 mountain stations from different regions of the world. They found that trends in minimum temperatures generally increased with elevation, while for the maximum temperatures the dependence on elevation was less clear with a pronounced warming between 500 and 1000 m, globally. The study by Pepin and Lundquist (2008) analysed more stations (1084) and a longer time period (1948-2002) focusing on mean annual temperatures. Though they found no significant correlation between the magnitude of the trend and the elevation, their analysis showed that the strongest warming signal was found around the 0°C isotherm, ascribing this behavior to the importance played by the snow/ice-albedo feedback. Many subsequent studies performed at regional level corroborated this finding (e.g. Palazzi et al., 2017). Ohmura (2012) analysed from 50 to 125 years of annual mean temperature timeseries at 56 stations from 10 mountainous regions of the world (the Alps, Kashmir, the Himalayas, Tibet, the Tianshans, the Qilianshans, the Japanese Archipelago, the Andes, the North American Cordillera and the Appalachians), finding that 65% of the analysed groups showed the largest trend of temperature change at the highest locations, 20% at an intermediate altitude between the top and the foot of mountains, and the remaining 15% at the lowest elevations. The annual trend was mostly affected by the cold season trend.

Wang et al. (2014) examined trends in mean annual temperatures and their dependence on elevation between 1961 and 2010 at a quite large number of stations around the globe, finding a significant amplification of warming rates with elevation in many regions including the Tibetan Plateau, the European Alps and the US Rocky Mountains. There are numerous studies conducted at the regional level, too, examining the available observations in a particular area/mountain range. The most striking observational evidence for EDW is certainly from the Asian mountains. The analysis of temperature data from 139 stations on and around the Tibetan Plateau (Yan and Liu 2014), for example, revealed that warming trend evaluated during the period 1961-2012 systematically increase with elevation for annual mean temperature, and that warming rates have increased in recent decades (Figure 1a of Pepin et al., 2015). Mean minimum temperatures also show EDW on an annual basis, as do mean temperatures in autumn and in winter. There was no strong elevational effect in other seasons, or for mean maximum temperatures, a result that is consistent with findings in other areas. In the Alpine region from the late 19<sup>th</sup> century until the end of the 20<sup>th</sup> century, temperatures have risen at a rate about twice as large as the northern-hemispheric average (Auer et al., 2007). Previous studies (Beniston et al., 1997) suggested that larger increases in average surface air temperature at higher elevations in the Alps occurred in winter and spring compared to other seasons, particularly in the Swiss Alps, mainly associated with a strong snow-albedo feedback. Another study focusing on the southern part of the Eastern Alps (the Trentino region), however, found that warming rates were larger at lower elevations in the period 1975-2010 and attributed this behavior to solar brightening and increased radiative forcing at lower elevations (Tudoroiu et al., 2016). In the Colorado Rocky mountains, EDW and its possible effects on snowpack characteristics and timing of seasonal melting, forests and vegetation have been documented in past studies. One of them (Diaz and Eischeid, 2007), for example, documented enhanced warming rates in the period 1987– 2006 with respect to the early 20<sup>th</sup> century above about 2000 m a.s.l. with trends exceeding by about 1°C the average temperature increase in the Western US. This and other studies (e.g., Daly et al., 2008; Williams et al., 2010; Clow, 2010; Pederson et al., 2011, 2013) assessed EDW in this region using measurements from the high-elevation Snowpack Telemetry (SNOTEL) network and related gridded climate products, though other authors (Oyler et al., 2015) subsequently highlighted possible inhomogeneities and issues related to this dataset.

### **2.3.2 Evidence of EDW in model simulations**

In spite of their coarse resolution, climate models allow to overcome some of the inadequacies inherent in all observing systems, particularly when trying to identify the main EDW mechanisms at work. In fact, the output of numerical models includes all the variables which potentially are drivers of EDW and which are difficult to measure at the same time in a given location. Moreover, models are run over long time periods to simulate both past conditions and future projections. Therefore, model simulations have been widely used to assess and understand EDW both in historical and future projections.

The literature reports some EDW studies using regional climate models (RCMs), whose fine scales are in principle more suitable to capture the effects of the complex mountain topography on climate processes than coarser resolution global climate models (GCMs).

Here are some examples of studies using RCMs. One paper by Giorgi et al. (1997) used a hydrostatic RCM at 50 km over the Alpine region and found enhanced warming rates in response to a doubling of CO<sub>2</sub> concentration with more pronounced changes at higher elevations particularly in winter and spring, mostly associated with a decrease in snowpack. The snow-albedo feedback was also found to be the main cause of the enhanced warming occurring in the minimum temperature at higher elevations, especially during winter, in the study by Im and Ahn (2011) where the elevational dependency of the temperature changes over Korea using a RCM at 20 km resolution was investigated. The study by Minder et al. (2018) explored the characteristics of EDW in the Rocky Mountains using the Weather Research and Forecasting Model (WRF) simulations at resolutions less or equal than 12 km and found very complex patterns of warming with elevation, including cases of warming nearly independent of height. They also found that warming is maximum in regions of maximum snow loss and albedo reduction, identifying, again, the snow-albedo feedback as the primary cause of EDW. At the same time, their simulations showed that EDW depends strongly on the adopted RCM configuration including the dependence not only on the spatial resolution but also on the land surface model used in the RCM.

In spite of the finer resolution of RCMs compared to GCMs (on average coarser than 120 km; Taylor et al., 2012), the majority of model studies performed so far on EDW is exactly based on the use of GCMs, both using a single GCM (e.g., Fyfe and Flato, 1999; Liu et al., 2009; Rangwala et al., 2010; Yan et al., 2016) or multi-model/multi-member ensembles (e.g., Rangwala et al., 2013, 2016; Palazzi et al., 2017). In a recent study, for example, Yan et al. (2016) performed specific experiments to test the sensitivity of the CCSM3 GCM to changes in CO<sub>2</sub> concentrations and found that the changes in snow depth and cloud cover in and around the Tibetan Plateau in response to CO<sub>2</sub> quadruplication would lead to EDW. Rangwala et al. (2013) analysed the CMIP5 GCMs up to 2100 and found that warming rates are projected to be amplified at higher altitudes with respect to the adjacent areas in the Tibetan Plateau and in the Rocky Mountains in North America, especially in the cold season. They found enhanced increases in the minimum temperature in the Tibetan Plateau related to increases in the downward longwave radiation and in the maximum temperature in the Rocky Mountains associated with snow reduction and snow-albedo feedbacks. Palazzi et al. (2017) investigated elevation-dependent warming in the Tibetan Plateau–Himalayas using a subset of the CMIP5 ensemble and found that changes in surface albedo, atmospheric humidity and downward longwave radiation are relevant factors for EDW in that area, with surface albedo being the leading driver.

We summarize here below the results of one recent study (Palazzi et al., 2019) which analyses EDW in three different mountain regions of the world – the Colorado Rocky Mountains, the Greater Alpine Region (GAR) and the Tibetan Plateau–Himalayas shown in Figure 3 - using one state-of-the-art Global Climate Model (EC-Earth version 3.1, Hazeleger et al., 2010, 2012). The results which we found for the GAR, in particular, are part of the expected outcomes of the NextData project and will be discussed in detail in this chapter.

The aim of that study was to investigate the impact of model spatial resolution on the representation of this phenomenon and to highlight possible differences in EDW and its causes in different mountain regions of the Northern Hemisphere. In fact, we used EC-Earth climate simulations at five different spatial resolutions, from ~ 125 to ~ 16 km, available for this specific set

of simulations. The coarsest of them, about 125 km, is the one typically used in state-of-the-art global climate model simulations (e.g. in the latest CMIP5 intercomparison project), while the finest, about 16 km, is a resolution typically used for numerical weather predictions.

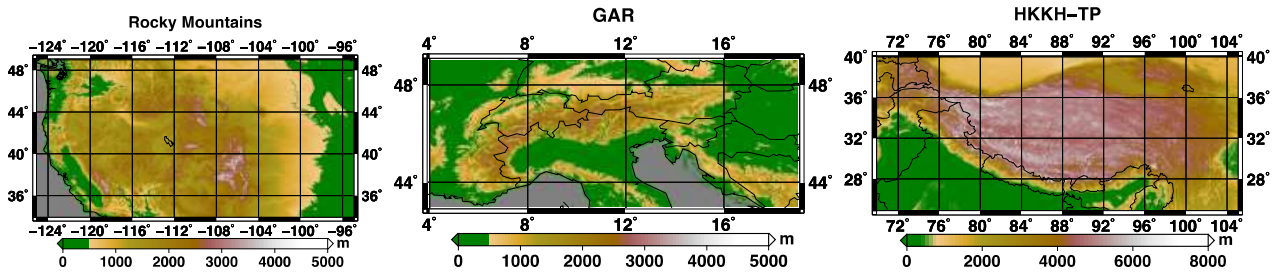


**Figure 3.** Topographic maps of the three study areas (left: Rocky Mountains; middle: Greater Alpine Region; right: Hindu Kush–Karakoram–Himalaya–Tibetan Plateau) from a high-resolution Digital Elevation Model at  $\sim 0.0167^\circ$  resolution. Green areas lie below 500 m a.s.l. and are excluded in our analysis (Palazzi et al., 2019).

That specific set of simulations with EC-Earth were performed in the framework of the PRACE project “Climate SPHINX” (Stochastic Physics High resolutionN eXperiments), whose detailed description can be found in Davini et al. (2017) and in the project web pages (<http://www.to.isac.cnr.it/sphinx/>). Briefly, these are atmosphere-only experiments extending for 30 years in the past (from 1979 to 2008) and 30 years in the future (from 2039 to 2068) using forcing conditions from the Representative Concentration Pathway emission scenario RCP 8.5 (Riahi et al., 2011), which assumes no stabilization in greenhouse gas emissions during the 21st century. For each resolution, more than one model member was produced. However, owing to computational costs, a different number of EC-Earth members is available for each resolution, from twenty (coarsest resolution) down to two (finest resolution). A peculiarity of the SPHINX experiment is that half of the members at each resolution was run including base physics while the other half using stochastic parameterizations (Davini et al., 2017), the latter being a way to include small-scale processes in coarse resolution without being computationally-demanding. These ensembles gave us the opportunity to gauge both the internal variability of the EC-Earth model and the uncertainty associated with the specific model chosen (either as model implement base physics and the model with stochastic parameterizations).

This model study showed that the more frequent drivers of EDW in the three northern hemispheric mountain regions (Rocky Mountains, GAR and Himalayas) and in the four seasons are the changes in albedo and in downward thermal radiation and this is reflected in both daytime and nighttime warming. In the GAR (and in the Tibetan Plateau-Himalayas), an additional driver is the change in specific humidity. A clear dependence on the resolution on the model ability in simulating the existence of EDW was not found, however in none of the regions. On the other hand, specific EDW characteristics such as its intensity and the relative role of different driving mechanisms may be different in simulations performed at different spatial resolutions. As an additional, interesting result, the role of internal climate variability was found to be significant in modulating the EDW signal, as suggested by the spread found in the multi-member ensemble of the EC-Earth experiments which were used.

As already pointed out in Section 2.2, the first step to assess EDW is to quantify a warming signal. In the study presented on here, this is evaluated as the difference between the 2039–2068 future



climatology and the 1979–2008 past climatology of the minimum and of the maximum daily temperature ( $\Delta t_{\text{asmin}}$ ,  $\Delta t_{\text{asmax}}$ ). The temperature change between the future and past climatology is evaluated on a seasonal basis using the standard definition of the seasons for the Northern Hemisphere mid-latitudes: winter (December–February, DJF), spring (March– May, MAM), summer (June–August, JJA), and autumn (September–November, SON).

The second step is to assess whether the warming signal in minimum and maximum temperatures exhibits a dependence on elevation and if the signal is statistically-significant. We calculate the slope obtained by linear regression of timeseries of daily minimum or maximum temperature against the model elevation. The regression is performed both at each grid point and using data averaged into elevational bands. The statistical significance of the linear slopes is assessed using a Student's t test, which tests against the null hypothesis that the coefficient of the regression is zero (no slope). We also explore a methodology based on grouping the temperature change data into elevation bins and then fitting the Probability Density Function (PDF) of the temperature changes evaluated for each bin with a LOcal regrESSion (LOESS) method. In fact, the uneven distribution of points at different elevations may have an impact on the slope evaluation and the dependence of the temperature changes with elevation may not be linear. Using the PDF solves the first issue while the LOESS regression would highlight possible departures from linearity. Only grid cells with elevation above 500 m a.s.l. are considered in order to reduce some of the influence of the coastal areas or of other areas generating potential interference, such as the Po Valley in the Greater Alpine Region.

Figures 4 and 5 show, for the minimum and maximum temperature respectively and for the GAR, in black the regression line evaluated using all data, in green the regression line evaluated fitting the average of the data (green dots) in each 100 m-thick elevational bin, and in blue a LOESS fitting curve. Purple shading indicates the probability density of a given minimum temperature change in each elevation bin. Figure 6 shows, for each model resolution (displayed along the x-axis) and season (each column plot), the value of the slope describing the linear relationship between either the minimum or maximum temperature change and the elevation (corresponding to the slope of the green line in Figures 4 and 5). Each grey circle indicates the output of one individual model member at each resolution, while the black circle denotes the multi-member mean. Empty symbols indicate elevational gradients of surface warming that are not statistically significant. Positive slopes in Figure 6 indicate EDW, while negative slopes highlight the situations in which there is still warming but it is larger at lower elevations (assuming a linear relationship) and we do not focus on this kind of occurrences. Finally, Table 1 summarizes the information provided in Figure 6.

In the Greater Alpine Region, EDW is detected in summer and autumn at the three finest resolutions, while in winter and spring it is detected only at the coarsest resolutions (T255 and T159 in winter, T159 in spring). The relationship between warming rates and elevation is well represented by a linear model, as clearly visible in Figures 4 and 5. Further, the PDF of the temperature change in each bin is well peaked around its mean value, which allows to have an unambiguous estimate of the warming expected at each elevation.

The season showing the most striking evidence of EDW in both  $t_{\text{asmin}}$  and  $t_{\text{asmax}}$  is autumn (this is true also for the Rocky Mountains and the Himalayas, which are not discussed in this report, see Palazzi et al., 2019 for details). In fact, the elevational gradients of warming rates in SON exhibit always a positive and statistically significant slope, except for  $t_{\text{asmax}}$  at t255 and t159 resolutions,

and the spread among the individual model realizations at each resolution is overall smaller than in the other seasons. EDW is not simulated for tasmin in DJF and in MAM: the statistically significant slopes which we found, in fact, are all negative. In some cases, we find considerable variability of the response among the ensemble members at a given resolution and, in a few cases, some members present both positive and negative slopes. We do not find any clear signal in the response of the different members run in this set of simulations to be directly ascribable to the two possible models used in SPHINX (i.e., the use of either base physics or stochastic parameterizations). This is visible in Figure 6 looking at the highest resolution (t1279) results, as the only two members available at this resolution, run either with or without stochastic parameterizations, do not provide significantly different EDW response.

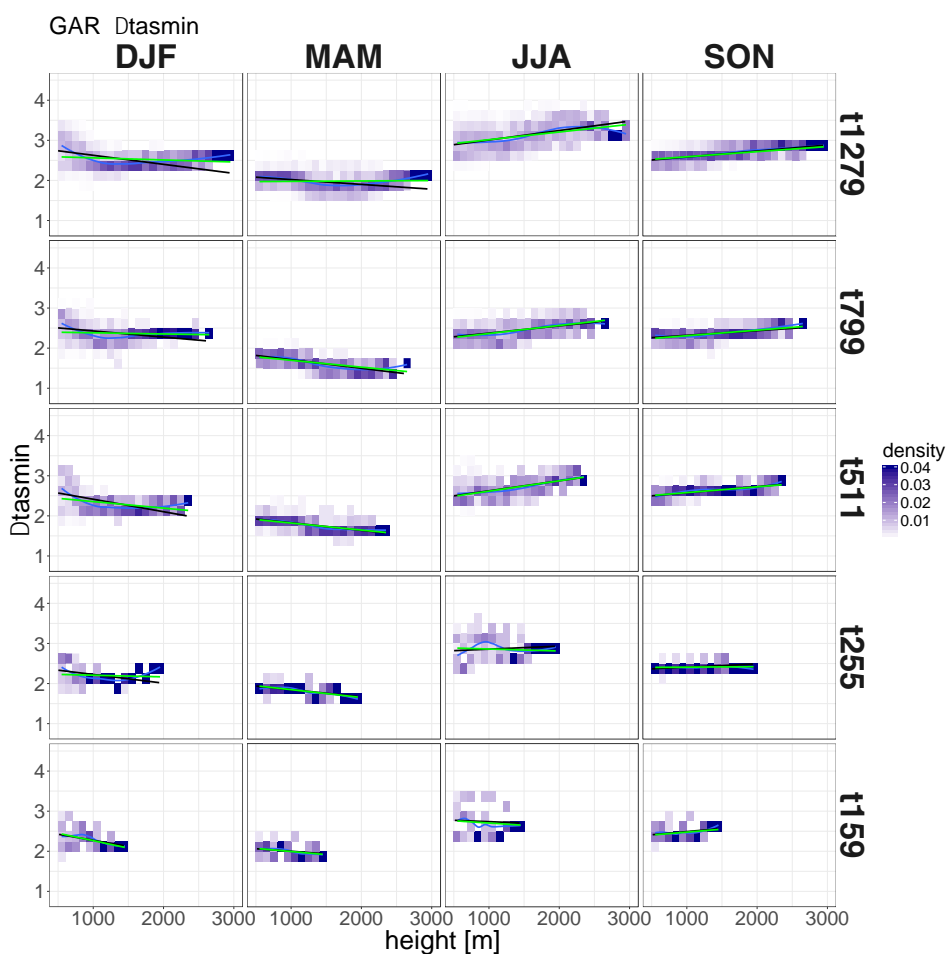


**Figure 4.** Dependence of minimum daily temperature (*tasmin*) on elevation for the Greater Alpine Region. The black line is the regression line evaluated using all data while the green line that evaluated fitting the average of the data (green dots) into each elevational bin. Superimposed is the PDFs of the temperature change calculated for each bin (shading). The LOESS curved fitting line is also shown in blue. From Palazzi et al., 2019 (supplementary material).

In order to identify the variables that may potentially contribute to EDW in the Greater Alpine Region we considered the factors whose changes may alter the surface energy balance and cause temperature variations, including surface albedo, surface downwelling longwave (thermal) and shortwave radiation, and near-surface specific humidity, as already suggested by the literature (e.g. Rangwala and Miller, 2012; Palazzi et al., 2017). We calculated the change between the average in the period 2039–2068 and the average in the period 1979–2008 of the possible EDW drivers (as

done for the temperatures) and, in particular, the absolute change for albedo ( $\Delta\text{albedo}$ ) and the fractional (or normalized) change for  $r_{\text{lds}}$ ,  $r_{\text{sds}}$ , and  $\text{huss}$  ( $\Delta r_{\text{lds}}/r_{\text{lds0}}$ ,  $\Delta r_{\text{sds}}/r_{\text{sds0}}$ ,  $\Delta \text{huss}/\text{huss0}$ ). Fractional changes are calculated relative to the averaged climatology between the mean in the years 1979–2008 and the mean in the years 2039–2068). In order for the variables listed above -  $\Delta\text{albedo}$ ,  $\Delta r_{\text{lds}}/r_{\text{lds0}}$ ,  $\Delta r_{\text{sds}}/r_{\text{sds0}}$ ,  $\Delta \text{huss}/\text{huss0}$  - to be actual EDW drivers, the following conditions have to be satisfied:

- 1) they have to exhibit a dependence on the elevation and the sign of that dependence has to be physically consistent with enhanced warming with elevation, and
- 2) they have to spatially correlate with temperature variations even if the dependence on elevation is removed.

Condition (1) implies that the changes in radiations ( $r_{\text{sds}}$ ,  $r_{\text{lds}}$ ) and in  $\text{huss}$  have to exhibit the same elevational dependence as the temperature change does: if these variables increase (decrease) also the temperature change increases (decreases). On the contrary, changes in albedo have to exhibit an elevational gradient of opposite sign, since an increase in albedo leads to a reduction of absorbed radiation at the surface and, therefore, to a decrease in surface warming. Basically, condition (1) ensures that the variation with altitude of a given variable and the altitudinal dependence of temperature changes are related with each other by some physical mechanisms. Condition (2) is essential to identify those variables which still (spatially) correlate with temperature changes independently of elevation.

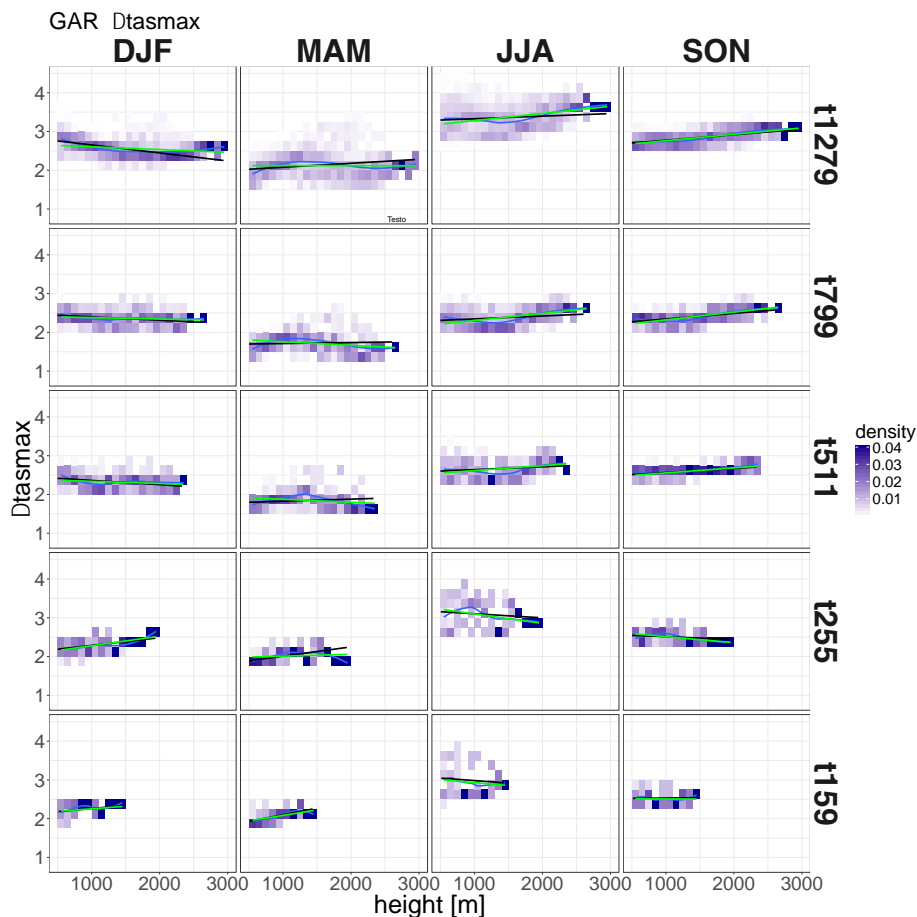


**Figure 5.** The same as Figure 3, for the maximum temperature ( $t_{\text{asmax}}$ ). From Palazzi et al., 2019 (supplementary material).

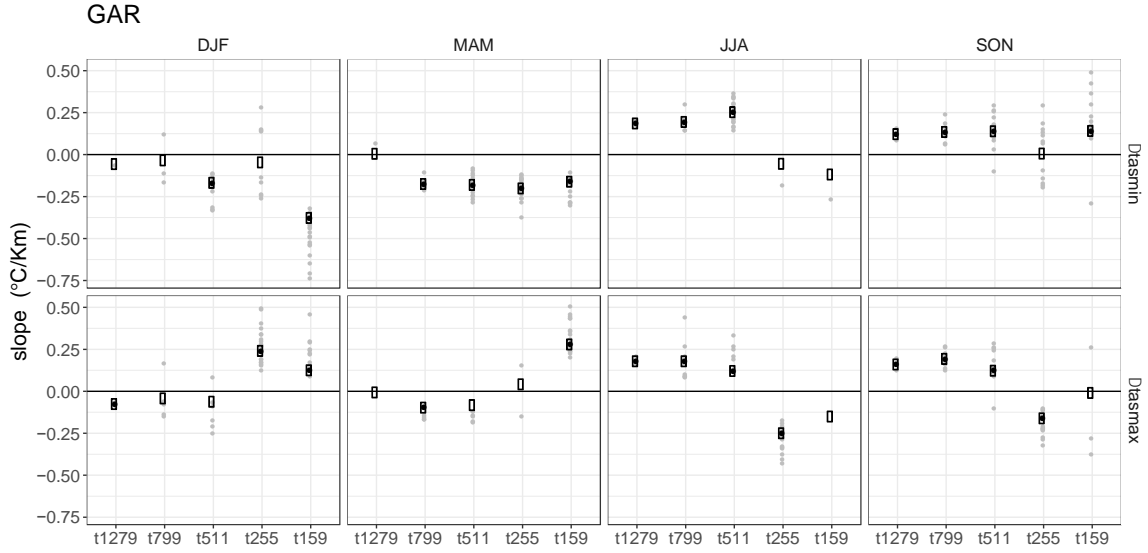


**Figure 6.** Elevational gradients of the seasonal temperature change in the Greater Alpine Region, for each ensemble member at different EC-Earth model resolutions. The minimum and maximum temperature changes are shown in the top and bottom panels, respectively, while different seasons are organized in the different columns. Each gray circle is the output of one individual model ensemble member at each resolution, while the black circle denotes the multi-member mean. The open symbols represent statistically non-significant elevational gradients of warming rates. From Palazzi et al., 2019.

	<i>tasmin</i>					<i>tasmax</i>				
	t1279	t799	t511	t255	t159	t1279	t799	t511	t255	t159
<b>DJF</b>	(N)	(N)	N	(N)	N	N	(N)	(N)	Y	Y
<b>MAM</b>	(Y)	N	N	N	N	(N)	N	(N)	(Y)	Y
<b>JJA</b>	Y	Y	Y	(N)	(N)	Y	Y	Y	N	(N)
<b>SON</b>	Y	Y	Y	(Y)	Y	Y	Y	Y	N	(N)

**Table 1.** Cases where EDW (i.e., enhanced warming rates with elevation) is detected or not detected (indicated by Y and N respectively). Parentheses indicate cases where the signal is not statistically significant.

To disentangle the relative importance of the identified EDW drivers in each season and region we set up a multiple linear regression model (see Eq. 1) in which the change in daily minimum or maximum temperature is the predictand and the possible drivers are the predictors. Predictors and the predictand are altitude-detrended, by removing the linear fit on elevation, and standardized, by dividing each change by its standard deviation over the whole spatial domain.

$$\Delta(tasmin, tasmax) = a_1 driver_1 + a_2 driver_2 + \dots + a_n driver_n + \eta \quad (1)$$

In Eq. 1 the drivers correspond to the variables that, among  $\Delta albedo$ ,  $\Delta rlds/rlds0$ ,  $\Delta rsds/rsds0$ , and  $\Delta huss/huss0$ , fulfil conditions (1) and (2) listed above. This approach allows to test all the possible combinations of the n predictors that lead to a different regression model. Overall, the possible regression models are  $(2n - 1)$  and their ability in predicting the temperature change is quantified by the coefficient of determination  $R^2$  that measures the proportion of the variance of the

predictand that they can explain: the closer  $R^2$  is to 1, the better the prediction is. At the same time, the value of  $R^2$  allows to quantify how much of the EDW response in the model is not explained by the predictors considered. By construction, the regression models including a larger number of predictors are associated with higher values of  $R^2$ . Therefore, to measure the relative quality of the regression models we use the Akaike information criterion corrected for finite sample sizes (AICc), which favors the models with less predictors and penalizes those with more (the lower the AICc, the better the model).

We analyse the role of the four variables, possible drivers of EDW ( $\Delta\text{albedo}$ ,  $\Delta\text{rlids}/\text{rlids0}$ ,  $\Delta\text{rsds}/\text{rsds0}$ ,  $\Delta\text{huss}/\text{huss0}$ ) in the GAR, in the different seasons and assessing whether model simulations performed at different spatial resolutions present different behaviours. From a practical point of view we proceed with the calculation of the three linear Pearson correlation coefficients described below, useful to check if the conditions (1) and (2) are fulfilled:

- $R_1$ , between either  $\Delta\text{tasmin}$  or  $\Delta\text{tasmax}$  and elevation, and its statistical significance, to highlight the cases with or without EDW.
- $R_2$ , between each of the four possible EDW drivers and elevation, and its statistical significance;
- $R_3$ , between the (minimum, maximum) temperature change and each of the four possible EDW drivers, and its statistical significance.  $R_3$  is calculated after having removed the dependence on elevation of each variable, which is obtained by considering the residuals compared to a linear fit respect to elevation.

A positive sign of  $R_2$  for  $\Delta\text{rlids}/\text{rlids0}$ ,  $\Delta\text{rsds}/\text{rsds0}$ ,  $\Delta\text{huss}/\text{huss0}$  and  $-\Delta\text{albedo}$  is physically consistent with EDW (i.e., with the condition  $R_1 > 0$ ). Therefore, having  $R_2$  greater than zero and statistically significant is one necessary condition for those variables to be actually drivers of EDW. For the variables that fulfil this condition we compute the correlation coefficient  $R_3$ , measuring their spatial correlation with the temperature change, after having detrended all variables for elevation. The  $R_3$  values are shown in Figure 7 for *tasmin* (left column) and *tasmax* (right column). Grey boxes indicate the cases in which there is no EDW or it is not statistically significant, based on the values of  $R_1$ , while white boxes identify the situations in which

- for a given variable,  $R_2$  is negative or not statistically- significant, which indicates that the variable certainly cannot be a driver of EDW. We recall that the condition  $R_2 < 0$  applies also to the change in albedo since we use  $-\Delta\text{albedo}$  in the calculations,
- the spatial correlation between a possible driver of EDW and the temperature change is negative.

Figure 7 thus indicates what are the possible drivers of future EDW in the GAR and how much they correlate (value of  $R_3$ ) with the change in the minimum and maximum temperature. The relative contribution to EDW of the different drivers can be assessed using the multiple linear regression model described by Eq. 1. Since we notice that the season showing the strongest evidence of EDW is SON, for simplicity in the following we discuss in detail the results of application of the multiple linear regression model for SON only. The other seasons are described in a more qualitative way instead. In the GAR, the three drivers of the changes in *tasmin* in JJA and SON (in DJF and MAM EC-Earth did not show EDW) are  $\Delta\text{albedo}$ ,  $\Delta\text{rlids}/\text{rlids0}$ , and  $\Delta\text{huss}/\text{huss0}$ . The only EC-Earth resolutions

which are able to identify the simultaneous contribution of all three drivers are T1279 and T799 and we apply the multiple linear regression model only for these two resolutions (and for SON). The results are summarized in Table 2, left columns. At T1279, the four models including  $\Delta rlds/rlds0$  as a predictor show the highest values of explained variance among the seven regression models. At T799 the first three models and the fifth in the rank include  $\Delta rlds/rlds0$ , the model combining  $\Delta albedo$  and  $\Delta huss/huss0$  ranking fourth. At both resolutions, among the three single-predictor models, the one with  $\Delta rlds/rlds0$  shows the highest R2. The three multi-predictor models including  $\Delta rlds/rlds0$  in conjunction with any other driver are capable of accounting for more than half the variance of the predictand at T799 (more than 20% at T1279). Therefore,  $\Delta rlds/rlds0$  is found, among the drivers which we considered, essential to drive the changes in tasmin in SON in the GAR.

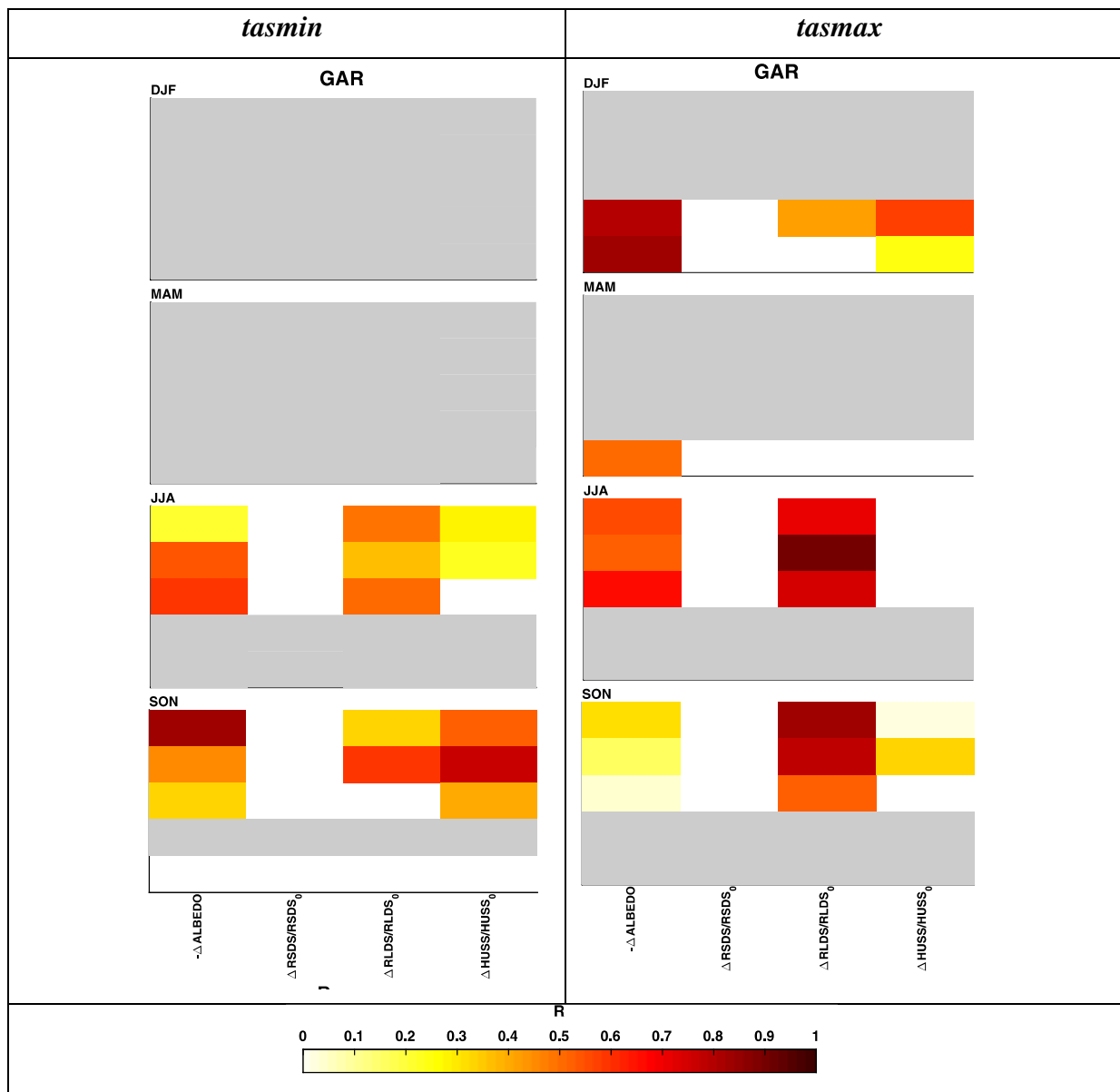


**Figure 6.** Correlation coefficient between each of the seven possible EDW drivers and the minimum temperature change on the left and the maximum temperature change on the right) in the four seasons. The drivers are displayed along the x-axis. Grey boxes indicate the cases in which there is no EDW or it is not statistically significant. White boxes identify the cases in which R2 is negative or not statistically-significant and the spatial correlation between a possible driver of EDW and the temperature change is negative. Modified from Palazzi et al., 2019.

As for the changes in tasmax, we identify as drivers in DJF  $\Delta\text{albedo}$ ,  $\Delta\text{rlids}/\text{rlds}_0$ , and  $\Delta\text{huss}/\text{huss}_0$  at T255 and  $\Delta\text{albedo}$  and  $\Delta\text{huss}/\text{huss}_0$  at T159. In JJA, the drivers are  $\Delta\text{albedo}$  and  $\Delta\text{rlids}/\text{rlds}_0$  and the signal is robust across all EC-Earth resolutions (T1279, T799, T511) at which EDW is found. In SON, the drivers are  $\Delta\text{albedo}$  and  $\Delta\text{rlids}/\text{rlds}_0$  at T511 and  $\Delta\text{albedo}$ ,  $\Delta\text{rlids}/\text{rlds}_0$  and  $\Delta\text{huss}/\text{huss}_0$  at T1279 and T799. For the latter two resolutions we discuss the results of application of the multiple linear regression model to study the relative contribution of the three identified drivers (see the right columns in Table 2).  $\Delta\text{huss}/\text{huss}_0$  emerges as the most important driver at T1279, while  $\Delta\text{albedo}$  is the most important driver at T799. In both cases the proportion of the maximum variance explained by the best-performing regression model is quite low (44% at T1279 and 41% at T799).

In general, our analysis shows that the more frequent EDW drivers in all seasons are the changes in albedo and in downward thermal radiation and this is reflected in both daytime and nighttime warming. It is clear that our picture omits other factors which may contribute to EDW in the different regions. It is interesting to observe that in the Alps, and at the coarsest horizontal resolutions only, a significant EDW signal related to albedo changes is observed in the DJF season. At the coarsest resolutions, the orography is smooth, and the highest elevations are not realistically represented in the climate model. This result seems to suggest that the “model’s highest elevations” might undergo an earlier (winter) transition from being snow covered to being snow free in the future in winter months. Of course this signal is an artifact typical of the coarsest resolutions and disappears at finer resolutions when the orography is represented with more accuracy. On the contrary, the finest resolutions are the only ones able to catch the change in albedo as an EDW driver in SON in the GAR. This result would suggest an added value of the finest resolution simulations in the Alpine area.

GAR, SON											
$\Delta(\text{tasmin}, \text{tasmax}) = a_1 \Delta\text{albedo} + a_2 \Delta\text{huss}/\text{huss}_0 + a_3 \Delta\text{rlids}/\text{rlds}_0$											
	Rank	$\Delta\text{tasmin}$					$\Delta\text{tasmax}$				
		$\Delta\text{albedo}$	$\frac{\Delta\text{huss}}{\text{huss}_0}$	$\frac{\Delta\text{rlids}}{\text{rlds}_0}$	$R^2$	AICc	$\Delta\text{albedo}$	$\frac{\Delta\text{huss}}{\text{huss}_0}$	$\frac{\Delta\text{rlids}}{\text{rlds}_0}$	$R^2$	AICc
		$a_1$	$a_2$	$a_3$			$a_1$	$a_2$	$a_3$		
T1279	1	-0.424	-0.170	0.456	0.356	-0.168	-0.511	-0.854	0.340	0.443	-0.361
	2	-0.354	-	0.385	0.339	-0.144	-0.500	-0.672	-	0.359	-0.221
	3	-	0.054	0.442	0.223	0.018	-	-0.584	0.323	0.250	-0.065
	4	-	-	0.470	0.221	0.020	-	-0.417	-	0.174	0.031
	5	-0.409	0.074	-	0.203	0.043	-0.156	-	-	0.024	0.197
	6	-0.447	-	-	0.200	0.047	-0.160	-	-0.017	0.025	0.198
	7	-	0.283	-	0.080	0.186	-	-	0.021	0.001	0.221
T799	1	-0.361	0.144	0.504	0.612	-0.295	-0.538	-0.376	0.546	0.411	-0.256
	2	-0.419	-	0.575	0.601	-0.270	-0.387	-	0.363	0.337	-0.140
	3	-	0.350	0.459	0.516	-0.076	-0.459	-	-	0.210	0.032
	4	-0.304	0.459	-	0.442	0.067	-0.476	-0.035	-	0.211	0.034
	5	-	-	0.658	0.432	0.084	-	-0.068	0.479	0.197	0.052
	6	-	0.610	-	0.373	0.184	-	-	0.440	0.193	0.053
	7	-0.533	-	-	0.284	0.313	-	0.203	-	0.041	0.226

**Table 2.** Application of the Eq. 1 including the three predictors ( $\Delta\text{albedo}$ ,  $\Delta\text{huss}/\text{huss}_0$  and  $\Delta\text{rlids}/\text{rlds}_0$ ) of the minimum (left) and maximum (right) temperature change in the GAR in SON. For each of the seven regression models obtained from the combination of the three predictors, the table shows the values of the regression coefficients  $a_1$  (referring to  $\Delta\text{albedo}$ ),  $a_2$  (referring to  $\Delta\text{huss}/\text{huss}_0$ ) and  $a_3$  (referring to  $\Delta\text{rlids}/\text{rlds}_0$ ), of the coefficient of determination  $R^2$  and of the AICc. See Palazzi et al., 2019.

Finally, it is important to stress that enhancing the spatial resolution in climate models may be crucial especially in complex topography, but also improvements in model parameterizations, particularly those involving surface processes in high-mountain areas, the snow-albedo and cloud-radiation feedbacks, may allow for a better simulation of EDW in the models. Considering the importance that mountains have as early warning indicators of the consequences of global warming, EDW is a phenomenon that calls for further research and efforts, both in terms of observations and of model simulations.

## **2.4 Causes of EDW**

Several mechanisms have been recognized as possible drivers of EDW. A full review of them can be found in Rangwala et al. (2012) and in Pepin et al. (2015), and references therein. These can arise either from an elevation-dependent change in drivers or in key variables such as snow and ice cover, clouds, water vapor amount, aerosols, soil moisture, or from an elevation-dependent sensitivity of surface warming to changes in these possible drivers. The considerations above suggest that EDW is a complex phenomenon, complicated by a number of variables which interact with each other, possibly giving rise to feedback mechanisms. All this, together with the limitations inherent in both high-altitude observations and in model simulations discussed above, makes it very difficult, but at the same time also very exciting, the study of this phenomenon. In the following, some of the main EDW causes investigated so far are discussed in more detail.

### **2.4.1 Snow/ice albedo feedback**

The snow/ice albedo feedback is among the strongest feedback loops active in the climate system, particularly important in cold regions. It is illustrated in simple way in Figure 7.

In response to a temperature increase, more snow or ice melts thus decreasing the local albedo, allowing for increased absorption of solar radiation and, by consequence, for an enhancement of the initial warming. Since this feedback modulates the surface absorption of incoming solar radiation, it is expected to affect primarily maximum temperatures. Nevertheless, it has been found that this feedback also acts in modulating nighttime minimum temperatures, especially when decreases in snow cover are accompanied by increases in soil moisture. This can, in turn, lead to a greater retention in the land surface of the solar energy absorbed during the day and, therefore, to an amplification of the longwave radiation release during the night (Rangwala et al., 2012). Ice-albedo feedback has been recognized as the most important EDW driver for both the maximum and the minimum temperature also by Palazzi et al. (2017), in a study focused on the Tibetan Plateau-Himalayas.



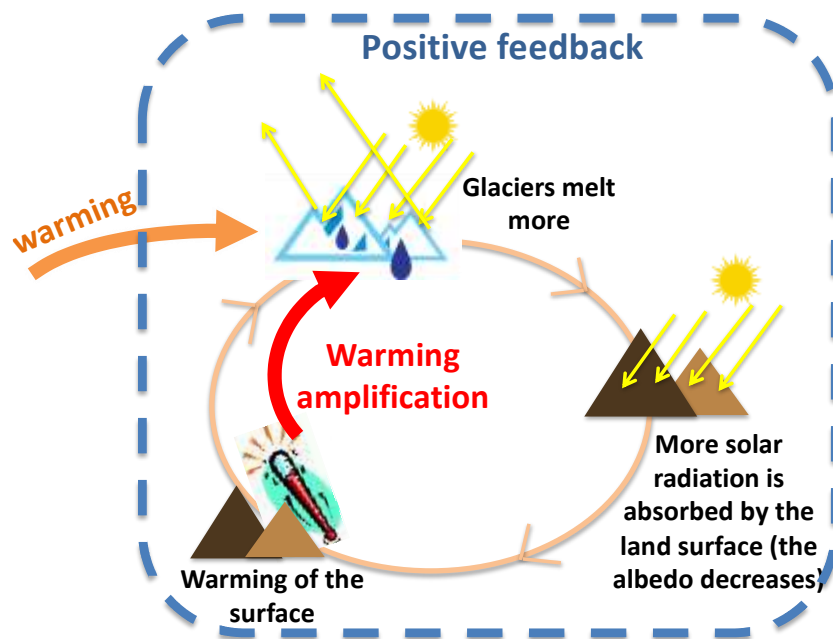


**Figure 7.** Sketch on how the ice/snow albedo positive feedback works, resulting in an amplification of an initial warming in high-elevation regions.

This feedback is most effective at elevations around the annual 0°C isotherm (Pepin and Lundquist, 2008, Palazzi et al., 2017, 2019), and it is expected to act predominantly at lower elevations earlier in the cold season while at higher elevations later on.

#### 2.4.2 Cloud cover

Clouds, and their related processes and feedbacks, are among the most (or probably the most) uncertain components of the climate system. Clouds affect both shortwave and longwave radiation and, as a consequence, their effect on the climate system is twofold. Some types of clouds are effective in reflecting shortwave radiation, which can lead to cooling, while others act like greenhouse gases by absorbing and re-emitting terrestrial longwave radiation, and thus can lead to warming. A decrease in cloud cover during the day is expected to enhance the maximum temperature, while a decrease in cloud cover during the night is expected to lower the minimum temperature.

To what extent can clouds contribute to EDW? Observational and model studies conducted over the Tibetan Plateau have shown that an increase in cloud cover during the night can lead to an increase in the minimum temperature and is among the main mechanisms responsible for EDW in the minimum temperature in this area (Wu, 2006).

Owing to the lack of long-term observational cloud datasets able to resolve their local impact on climate, quantifying cloud feedbacks still remain challenging and mostly rely on the use of numerical models of the climate system. Liu et al. (2009), for example, examined more than a hundred of weather stations and the output of a high-resolution climate model simulation under a future greenhouse-warming scenario finding that the increase in monthly minimum temperatures was greater at higher elevations in the Tibetan Plateau. They recognized in cloud-radiation effects the mechanisms responsible for this elevational dependence.

### **2.4.3 Water vapor modulation of longwave heating**

A warmer atmosphere is able to hold more water vapor. Though not directly emitted by human activities, water vapor is a powerful greenhouse gas and, as such, it participates in one of the most important feedback loops active in the climate system, the water vapor/greenhouse gas feedback: more water vapour in the atmosphere leads to more warming, more warming leads to more water vapour, and so on and so forth.

Increases in surface specific humidity have been suggested to be partly responsible for a rapid increase in surface warming in the Tibetan Plateau (Rangwala et al., 2009, 2010) in the late 20th century. This is related to the relationship between the increases in specific humidity and the increases in downward longwave radiation (DLR), which produces a surface warming.

Although increases in downward longwave radiation associated with increasing specific humidity occur globally, the sensitivity is non-linear and it is enhanced when the initial humidity is low as is commonly found at high elevations during the cold season. DLR, in particular, has large sensitivities to specific humidity when its concentration is below 5 g/kg. Such low values occur during the cold season and more widely at higher elevations. The same results were found by Rangwala et al. (2010) for the Tibetan Plateau.

### **2.4.4 Aerosols**

Absorbing aerosols like black carbon (soot) and dust are additional contributors to warming. During the boreal spring, an atmospheric layer of dust from deserts and locally-emitted black carbon can be found up to 5 km high in the Indo-Gangetic Plain against the foothills of the Himalayas and Tibetan Plateau (Ramanathan and Carmichael, 2008). Such a layer is able to absorb solar radiation and warm the mid-troposphere, which in turn increases the rate of spring snowmelt and leads to enhanced warming owing to the associated positive feedback.

In their review paper, Ramanathan and Carmichael (2008) suggested that black carbon in the Himalayan Mountains arising from anthropogenic activities might be responsible for half the total warming there during the last several decades. Because black carbon affects the radiation both absorbing solar radiation in the troposphere and decreasing surface albedo when deposited on snow or ice, it is very difficult to assess its effect on elevation-dependent warming. Depending on the elevation at which black carbon is deposited it could either contribute to enhanced or reduced warming with elevation during the melt season.

Similar to black carbon, dust also absorbs radiation within the atmosphere and reduces surface albedo when deposited on snow; similarly to black carbon, however, the impact of dust on EDW will depend on the elevation at which it is deposited.

## **2.5 Open issues**

Elevation-dependent warming is an issue which needs more systematic investigation. Part of the problem is that there is no universally agreed or standardized way to face it. Different researchers have posed slightly different ways of answering the question of whether mountains are warming faster than lowland areas, using different types of data and different methods of analysis.

*Which temperature one is usually dealing with?*

Detecting a signal of EDW first implies detecting temperature. One of the issues is exactly which temperature one is dealing with. Usually, temperature is intended to be 2 meter air temperature, that is what is usually measured by meteorological stations. This variable is what is actually available classified as surface temperature in most climate dataset and what is stored in the output of numerical climate model simulations as “surface air temperature (tas)”. However, in other research fields, like ecology or ecosystem research, one may be rather more interested in surface (skin) temperature, which is actually what is “felt” by living organisms. Analysis of satellite data generates the skin temperature (land surface temperature, LST), which is however different from near surface air temperature, in terms of physical nature and level of uncertainty inherent in the measurement of each parameter.

#### *Standardized and agreed methodology to assess EDW*

A universal method of defining and quantifying EDW in both observations and model simulations is needed. Researchers have used different data and different methodologies to investigate the elevational dependency of warming rates. Data sources include surface stations, model data, reanalysis data, radiosondes, satellite data. Although there are differences, most authors generate time series at locations of a given elevation and then extract the trend in this time series. Some authors create composite time series over an area (averaging a certain elevation), others trends at individual points.

There is no agreement on the length of the time period to be considered (though having at least 30 years should be the minimum requirement), or indeed whether there should be a composite regional series or lots of series at points of different elevations which are compared. Trends are usually quantified using some sort of regression line. The simplest method is the slope of the least squares regression line fitted to the time series, and then expressed in °C/decade. Linearity is an approximation.

There has also been a lack of consistency in the methods and data used to quantify the rate and patterns of warming. Differences in the time periods examined, the stations compared, the elevational range selected, and the temporal resolution of the data (that is, daily versus monthly or annual temperatures) all vary and thus contribute to differences in trends. Many studies are relatively short (less than 50 years) and so strong interdecadal variability often contributes to observed trends. Although some data homogenization has been achieved for station records in Europe and North America, there is a particular problem with the mountain data in the tropics, which is both sparse and inhomogeneous.

#### **2.5.1 Issues in observations and model simulations**

EDW is a complex process, both to measure and to model, and complicated by different factors. On the observational side, a homogeneous and dense network of meteorological stations would be required to clearly document the rate and the spatial distribution of warming as a function of elevation, but this is not the situation most commonly encountered in high-altitude regions.

The number of high-elevation stations providing long-term records (longer than at least 20 years) is still not adequate to allow evaluating statistically significant temporal trends, which is the first step

for the assessment and quantification of EDW. Mountain observations are known to be biased by altitude, since most in-situ stations are installed in valleys rather than on mountain slopes and on the tops, which represents an additional source of uncertainty.

Monitoring of land surface temperatures (LST) from satellite is another possible approach for studying EDW. The clear advantage of satellite observations over in-situ station data is their homogeneous spatial and temporal coverage; the disadvantage is that their temporal coverage is usually shorter than that provided by station records and less suitable for detecting climatic trends and their statistical significance. These data are also still poorly validated in high-elevation regions where cloud occurrence represents an obstacle for satellite monitoring and data interpretation. Model simulations are not affected by many of the inadequacies inherent in all kinds of observations, such as sparseness and limited temporal extension of the data, and they represent a very useful laboratory to investigate the possible mechanisms responsible for EDW. In fact, the output of numerical models includes all the variables, and their dynamical and physically-based relations, needed to build a picture of the EDW drivers, at a given spatial and temporal resolution, and long simulations can be run both to reproduce the past and to study future projections. Models, even RCMs, are generally limited in spatial resolution and require observational data for validation, making it difficult to be sure that simulations are accurate enough to be confident on future projections. Model resolution plays an important role for EDW. It is important to stress, however, that enhancing the spatial resolution in climate models may be crucial especially in complex topography, but also improvements in model parameterizations, particularly those involving surface processes in high-mountain areas, the snow-albedo and cloud-radiation feedbacks, may allow for a better simulation of EDW in the models (Palazzi et al., 2019).

## **2.6. Conclusions**

More research is needed to understand the complexity of mountain regions and, in particular, the EDW phenomenon and its driving mechanisms. The model studies performed so far found that the change in surface albedo turns out to be one of the main driving factors for EDW, suggesting the urgency of further developing models of those Earth system components which affect albedo, such as snow cover and glaciers. Proper simulation of snow cover requires appropriate simulation of precipitation and especially of snowfall and, by consequence, of clouds and cloud dynamics, which is one of the subgrid-scale phenomena in state-of-the-art GCMs, requiring the implementation of parameterisations. Also, proper parameterizations for the dependence of snow albedo on snow age, depth, terrain characteristics, aerosol deposition and others are of major importance.

Modelling glaciers, their dynamics, and the effects of climate change on them is as complex as crucial, too. Glacier expansion and retreat depend on the balance between accumulation and ablation and, therefore, winter snowfall and summer temperatures are key ingredients to assess the future glacier conditions. There is still a deficiency in the way climate models represent snow and ice albedo, which is mentioned as one of the main causes for the cold bias that still affects many GCM simulations. These variables are land fields and are produced by the land vegetation models that are coupled to the other model components in the state-of-the-art Earth System models. Therefore, improving the land-surface models would lead to a better description of the high-

mountain cryosphere system. Besides that, the use of finer resolution models would be useful to depict the complex topography of mountain regions in a more realistic way and therefore improve the way the models represent the changes of snow at ground.

## References

- Auer I., Böhm R., Jurkovic A., Lipa W., Orlik A., Potzmann R., Schöner W., Ungersböck M., Matulla C., Briffa K., Jones P., Efthymiadis D., Brunetti M., Nanni T., Maugeri M., Mercalli L., Mestre O., Moisselin J., Begert M., Müller-Westermeier G., Kveton V., Bochnicek O., Stastny P., Lapin M., Szalai S., Szentimrey T., Cegnar T., Dolinar M., Gajic-Capka M., Zaninovic K., Majstorovic Z., Nieplova E., 2007. HISTALP—historical instrumental climatological surface time series of the Greater Alpine Region. *Int. J. Climatol.*, 27:17-46. doi:10.1002/joc.1377.
- Barry R., 2008. *Mountain Weather and Climate*. Cambridge: Cambridge University Press. doi:10.1017/CBO9780511754753.
- Beniston M., 1997. Variations of Snow Depth and Duration in the Swiss Alps Over the Last 50 Years: Links to Changes in Large-Scale Climatic Forcings. In: Diaz H.F., Beniston M., Bradley R.S. (eds) *Climatic Change at High Elevation Sites*. Springer, Dordrecht.
- Chapin III F. S., Sturm M., Sertreze M. C., MCFadden J. P., Key J. R., Lloyd A. H., MCGuire A. D., Rupp T. S., Lynch A. H., Schimel J. P., Beringer J., Chapman W. L., Epstein H. E., Euskirchen E. S., Hinzman L. D., Jia G., Ping C.-L., Tape K. D., Thompson C. D. C., Walker D. A., Welker J. M., 2005. Role of Land-Surface Changes in Arctic Summer Warming, *Science* 657-660.
- Clow D. W., 2010. Changes in the timing of snowmelt and streamflow in Colorado: a response to recent warming. *J. Clim.* 23:2293–2306. <https://doi.org/10.1175/2009JCLI2951.1>.
- Daly C., Halbleib M., Smith J. I., Gibson W. P., Doggett M. K., Taylor G. H., Curtis J., Pasteris P. P., 2008. Physiographically sensitive mapping of climatological temperature and precipitation across the conterminous United States. *Int. J. Climatol.* 28:2031–2064. <https://doi.org/10.1002/joc.1688>.
- Davini P., von Hardenberg J., Corti S., Christensen H. M., Juricke S., Subramanian A., Watson P. A. G., Weisheimer A., Palmer T. N., 2017. Climate SPHINX: evaluating the impact of resolution and stochastic physics parameterisations in the EC-Earth global climate model. *Geosci. Model. Dev.* 10:1383–1402. <https://doi.org/10.5194/gmd-10-1383-2017>.
- Diaz H. F., Bradley R. S., 1997. Temperature variations during the last century at high elevation sites. *Climatic Change* 36:253-279.
- Diaz H.F., Eischeid J. K., 2007. Disappearing “Alpine Tundra” Koppen Climatic Type in the Western United States. *Geophysical Research Letters*, 34, L18707, <http://dx.doi.org/10.1029/2007gl031253>.
- Fyfe J. C., Flato J. M., 1999. Enhanced climate change and its detection over the Rocky Mountains. *J. Clim.* 12:230–243. <https://doi.org/10.1175/1520-0442-12.1.230>.
- Giorgi F., Hurrell J. W., Marinucci M. R., Beniston M., 1997. Elevation dependency of the surface climate change signal: a model study. *J. Clim.* 10:288–296. [https://doi.org/10.1175/1520-0442\(1997\)010%3c0288:EDOTSC%3e2.0.CO;2](https://doi.org/10.1175/1520-0442(1997)010%3c0288:EDOTSC%3e2.0.CO;2).
- Hansen J., Ruedy R., Sato M., Lo K., 2010. Global surface temperature change, *Rev. Geophys.*, 48, RG4004, doi:10.1029/2010RG000345.

- Hazeleger W., Severijns C., Semmler T., Ștefănescu S., Yang S., Wang X., Wyser K., Dutra E., Baldasano J. M., Bintanja R., Bougeault P., Cabalero R., Ekman A. M. L., Christensen J. H., van den Hurk B., Jimenez P., Jones C., Källberg P., Koenigk T., McGrath R., Miranda P., Van Noije T., Palmer T., Parodi J. A., Schmith T., Selten F., Storelvmo T., Sterl A., Tapamo H., Vancoppenolle M., Viterbo P., Willén U., 2010. EC-Earth: a seamless earth-system prediction approach in action. *Bull. Am. Meteorol. Soc.* 91:1357–1363. <https://doi.org/10.1175/2010BAMS2877.1>.
- Hazeleger W., Wang X., Severijns C., Ștefănescu S., Bintanja R., Sterl A., Wyser K., Semmler T., Yang S., van den Hurk B., van Noije T., van der Linden E., van der Wiel K., 2010. EC-Earth V2.2: description and validation of a new seamless earth system prediction model. *Clim. Dyn.* 39:2611–2629. <https://doi.org/10.1007/s00382-011-1228-5>.
- Im E.-S., Ahn J.-B., 2011. On the elevation dependency of present-day climate and future change over Korea from a high resolution regional climate simulation. *J. Meteorol. Soc. Japan* 89:89–100. <https://doi.org/10.2151/jmsj.2011-106>.
- IPCC, 2013 Climate Change 2013: The Physical Science Basis. Contribution of Working Group I to the Fifth Assessment Report of the Intergovernmental Panel on Climate Change [Stocker, T.F., D. Qin, G.-K. Plattner, M. Tignor, S.K. Allen, J. Boschung, A. Nauels, Y. Xia, V. Bex and P.M. Midgley (eds.)]. Cambridge University Press, Cambridge, United Kingdom and New York, NY, USA, 1535 pp.
- Liu X., Chen B., 2000. Climatic warming in the Tibetan Plateau during recent decades. *Int. J. Climatol.* 20:1729–1742. [https://doi.org/10.1002/1097-0088\(20001130\)20:14%3c1729::AID-JOC556%3e3.0.CO;2-Y](https://doi.org/10.1002/1097-0088(20001130)20:14%3c1729::AID-JOC556%3e3.0.CO;2-Y).
- Liu X., Cheng Z., Yan L., Yin Z.-Y., 2009. Elevation dependency of recent and future minimum surface air temperature trends in the Tibetan Plateau and its surroundings. *Global Planet Chang* 68:164–174. <https://doi.org/10.1016/j.gloplacha.2009.03.017>.
- Minder J. R., Letcher T. W., Liu C., 2018. The character and causes of elevation-dependent warming in high-resolution simulations of Rocky Mountain climate change. *J. Clim.* 31:2093–2113. <https://doi.org/10.1175/JCLI-D-17-0321.1>.
- Ohmura A., 2012. Enhanced temperature variability in high-altitude climate change. *Theor. Appl. Climatol.*, 110:499, <https://doi.org/10.1007/s00704-012-0687-x>.
- Oyler J. W., Dobrowski S. Z., Ballantyne A. P., Klene A. E., Running S. W., 2015. Artificial amplification of warming trends across the mountains of the western United States. *Geophys. Res. Lett.* 42:153–161. <https://doi.org/10.1002/2014GL062803>.
- Palazzi E., Filippi L., von Hardenberg J., 2017. Insights into elevation-dependent warming in the Tibetan Plateau–Himalayas from CMIP5 model simulations. *Clim. Dyn.* 48(11–12):3991–4008. <https://doi.org/10.1007/s00382-016-3316-z>.
- Palazzi E., Mortarini L., Terzago S., von Hardenberg J., 2019. Elevation-dependent warming in global climate model simulations at high spatial resolution. *Clim. Dyn.* 52:2685. <https://doi.org/10.1007/s00382-018-4287-z>, 2019.
- Pederson G. T., Betancourt J. L., McCabe G. J., 2013. Regional patterns and proximal causes of the recent snowpack decline in the Rocky Mountains, US. *Geophys Res Lett* 40:1811–1816. <https://doi.org/10.1002/grl.50424>.
- Pepin N. C., Lundquist J. D., 2008. Temperature trends at high elevations: patterns across the globe. *Geophys. Res. Lett.* 35:L14701. <https://doi.org/10.1029/2008GL034026>.

- Pepin N., Bradley R. S., Diaz H. F., Baraer M., Caceres E. B., Forsythe N., Fowler H., Greenwood G., Hashmi M. Z., Liu X. D., Miller J. R., Ning L., Ohmura A., Palazzi E., Rangwala I., Schöner W., Severskiy I., Shahgedanova M., Wang M. B., Williamson S. N., Yang D. Q., 2015. Elevation-dependent warming in mountain regions of the world. *Nature Climate Change*, 5, 424, <https://doi.org/10.1038/nclimate2563>.
- Qin J., Yang K., Liang S., Guo X., 2009. The altitudinal dependence of recent rapid warming over the Tibetan Plateau. *Clim. Chang.* 97:321–327. <https://doi.org/10.1007/s10584-009-9733-9>.
- Ramanathan V., Carmichael G., 2008. Global and regional climate changes due to black carbon, *Nature Geoscience* 1:221–227.
- Rangwala I., Miller J. R., Russell G. L., Xu M., 2010. Using a global climate model to evaluate the influences of water vapor, snow cover and atmospheric aerosol on warming in the Tibetan Plateau during the twenty-first century. *Clim. Dyn.* 34:859–872. <https://doi.org/10.1007/s00382-009-0564-1>.
- Rangwala I., Barsugli J., Cozzetto K., Neff J., Prairie J., 2012. Mid-21st century projections in temperature extremes in the southern Colorado Rocky Mountains from regional climate models. *Clim. Dyn.* doi:10.1007/s00382-011-1282-z.
- Rangwala I., Sinsky E., Miller R. J., 2013. Amplified warming projections for high altitude regions of the Northern hemisphere mid-latitudes from CMIP5 models. *Environ. Res. Lett.* 8:024040. <https://doi.org/10.1088/1748-9326/8/2/024040>.
- Rangwala I., Sinsky E., Miller R. J., 2016. Variability in projected elevation dependent warming in boreal midlatitude winter in CMIP5 climate models and its potential drivers. *Clim. Dyn.* 46(7):2115-2122. <https://doi.org/10.1007/s00382-015-2692-0>.
- Riahi K., Rao S., Krey V., Cho C., Chirkov V., Fischer G., Kindermann G., Nakicenovic N., Rafaj P., 2011. RCP 8.5—a scenario of comparatively high greenhouse gas emissions. *Clim. Chang.* 109:33–57. <https://doi.org/10.1007/s10584-011-0149-y>.
- Serreze M. C., Francis J. A., 2006. The Arctic Amplification Debate. *Climatic Change*, 76:241-264. <https://doi.org/10.1007/s10584-005-9017-y>.
- Serreze M. V., Barry R. G., 2011. Processes and impacts of Arctic amplification: A research synthesis. *Global and Planetary Change*, 77(1–2):85-96, ISSN 0921-8181, <https://doi.org/10.1016/j.gloplacha.2011.03.004>.
- Taylor K. E., Stouffer R. J., Meehl G. A., 2012. An overview of CMIP5 and the experiment design. *Bull. Am. Meteorol. Soc.* 93:485–498. <https://doi.org/10.1175/BAMS-D-11-00094.1>.
- Tudoroiu M., Eccel E., Gioli B., Gianelle D., Schume H., Genesio L., Miglietta F., 2016. Negative elevation-dependent warming trend in the Eastern Alps. *Environ. Res. Lett.* 11 044021.
- Vuille M., Bradley R. S., Werner M., Keimig F., 2003. 20th Century climate change in the tropical Andes: observations and model results. *Clim. Chang.* 59:75. <https://doi.org/10.1023/A:1024406427519>.
- Wang Q., Fan X., Wang M., 2014. Recent warming amplification over high elevation regions across the globe. *Clim. Dyn.*, 43:87. <https://doi.org/10.1007/s00382-013-1889-3>.
- Williams A. P., Allen C. D., Millar C. I., Swetnam T. W., Michaelsen J., Still C. J., Leavitt S. W., 2017. Forest responses to increasing aridity and warmth in the southwestern United States. *Proc. Natl. Acad. Sci.* 107:21289–21294. <https://doi.org/10.1073/pnas.0914211107>.

Yan L., Liu X., 2014. Has climatic warming over the Tibetan Plateau paused or continued in recent years? *J. Earth Ocean Atmos. Sci.* 1:13–28.

Yan L., Liu Z., Chen G., Kutzbach J. E., Liu X., 2016. Mechanisms of elevation-dependent warming over the Tibetan plateau in quadrupled CO<sub>2</sub> experiments. *Clim. Chang.* 135:509–519. <https://doi.org/10.1007/s10584-016-1599-z>.